The impact of elliptical deformations for optimizing the performance of dual-core fluorine-doped photonic crystal fiber couplers

Shailendra K. Varshney, Nikolaos J. Florous, Kunimasa Saitoh, and Masanori Koshiba

Division of Media and Network Technologies, Hokkaido University, Sapporo 060-0814, Japan
skvarshney_10@yahoo.co.uk

Abstract: In this paper we study the impact of elliptically-deformed features such as cladding air-holes and elliptically-modulated cores, as ingredients for optimizing the coupling characteristics of dual-core fluorine-doped photonic crystal fiber (PCF) couplers. We provide a detailed numerical investigation by using a trial and error approach for optimizing the propagation characteristics of fluorine-doped PCF couplers. Typical characteristics of the newly proposed PCF coupler structure are: wavelength-flattened coupling characteristics between 0.7 μm and 1.6 μm wavelength range, coupling efficiency of 50±1 % from 0.9 μm to 1.6 μm, and a reasonably small coupling length of 1.3 cm. In addition we have elaborately derived the design parameters so that our proposed dual-core PCF coupler exhibits polarization-insensitive characteristics verified by using a full-vectorial beam propagation method. The proposed dual-core PCF can be effectively used as a 3-dB coupler, over a wide wavelength range.

OCIS codes: (060.2430) Fibers, single mode; (060.2330) Fiber optics communications; (999.9999) Photonic crystal fibers

References and Links

1. T.A. Birks, J.C. Knight, and P.St.J. Russell, "Endlessly single-mode photonic crystal fiber," Opt. Lett. **22**, 961-963 (1997).
2. A. Bjarklev, J. Broeng, and A.S. Bjarklev, *Photonic Crystal Fibres*, (Kulwer Academic Publishers 2003).
3. B.J Mangan, J. Arriaga, T.A. Birks, J.C. Knight, and P.St.J. Russell, "Fundamental-mode cutoff in a photonic crystal fiber with a depressed-index core," Opt. Lett. **26**, 1469-1471 (2001).
4. J. Laegsgaard, O. Bang, and A. Bjarklev, "Photonic crystal fiber design for broadband directional coupling," Opt. Lett. **29**, 2473-2475 (2004).
5. B.J. Mangan, J.C. Knight, T.A. Birks, P.St.J. Russell, and A.H. Greenaway, "Experimental study of dual-core photonic crystal fiber," Electron. Lett. **36**, 1358-1359 (2000).
6. F. Fogli, L. Saccomandi, P. Bassi, G. Bellanca, and S. Trillo, "Full vectorial BPM modeling of index-guiding photonic crystal fibers and couplers," Opt. Express **10**, 54-59 (2002). http://oe.osa.org/abstract.cfm?id=67643
7. K. Saitoh, Y. Sato, and M. Koshiba, "Coupling characteristics of dual-core photonic crystal fiber couplers," Opt. Express **11**, 3188-3195 (2003). http://oe.osa.org/abstract.cfm?id=78078
8. W.E.P Padden, M.A.van Eijkelenborg, A. Argyros, and N.A. Issa, "Coupling in twin-core microstructured polymer optical fiber," Appl. Phys. Lett. **84**, 1689-1691 (2004).
9. L. Zhang and C. Yang, "Polarization-dependent coupling in twin-core photonic crystal fibers," J. Lightwave Technol. **22**, 1367-1373 (2004).
10. N. Florous, K. Saitoh, and M. Koshiba, "A novel approach for designing photonic crystal fiber splitters with polarization-independent propagation characteristics," Opt. Express **13**, 7365-7373 (2005). http://oe.osa.org/abstract.cfm?id=85438
11. K. Saitoh and M. Koshiba, "Full-vectorial imaginary-distance beam propagation method based on a finite element scheme: Application to photonic crystal fibers," IEEE J. Quantum Electron. **38**, 927-933 (2002).
12. K. Saitoh and M. Koshiba, "Full-vectorial finite element beam propagation method with perfectly matched layers for anisotropic waveguides," J. Lightwave Technol. **19**, 405-413 (2001).
13. M.J. Steel, and R.M. Osgood, "Polarization and dispersive properties of elliptical-hole photonic crystal fibers," J. Lightwave Technol. **19**, 495-502 (2001).

14. N. Florous and M. Koshiba, "Virtual boundary method for the analysis of elliptically cross-sectional photonic crystal fibers with elliptical pores," J. Lightwave Technol. **23**, 1763-1773 (2005).
15. F. Poletti, V. Finazzi, T.M. Monro, N.G.R Broderick, V. Tse, and D.J. Richardson, "Inverse design and fabrication tolerances of ultra-flattened dispersion holey fibers," Opt. Express **13**, 3728-3736 (2005). http://oe.osa.org/abstract.cfm?id=83819
16. N.A. Issa, M.A. Eijkelenborg, M. Fellew, F. Cox, G. Henry, and C.J. Large, "Fabrication and study of microstructured optical fibers with elliptical holes," Opt. Lett. **29**, 1336-1338 (2004).
17. T. Yamamoto, H. Kubota, S. Kawanishi, M. Tanaka, and S. Yamaguchi, "Super continuum generation at 1.55 μm in a dispersion-flattened polarization-maintaining photonic crystal fiber," Opt. Express **11**, 1537-1540 (2003). http://oe.osa.org/abstract.cfm?id=72896
18. S. G. Leon-Saval, T. A. Birks, N.Y. Joly, A. K. George, W. J. Wadsworth, G. Kakarantzas, and P.St.J. Russell, "Splice-free interfacing of photonic crystal fibers," Opt. Lett. **30**, 1629-1631 (2005).
19. H.C. Nguyen, B. T. Kuhlmey, M.J. Steel, C. L. Smith, E. C. Magi, R.C. McPhedran, and B.J. Eggleton, "Leakage of the fundamental mode in photonic crystal fiber tapers," Opt. Lett. **30**, 1123-1125 (2005).

1. Introduction

Over the last decade, an exponential growth has been observed in theoretical and practical implementation of photonic crystal fibers (PCFs), due to their remarkable properties such as, wide-band single mode operation [1], large effective mode area, high nonlinearities, and overall controlled dispersion properties [2]. The presence of air-holes in the cladding imparts intriguing properties to PCFs, which generally arises due to a strong wavelength-dependent cladding index.

Index-guiding PCFs, also known as holey fibers have particularly attracted considerably attention from the optical scientific community. One of the appealing properties of PCFs is the fact that they can possess dispersion properties significantly different than those of the conventional optical fibers, because their artificially-periodic cladding consisting of micrometer-sized air-holes allows the flexible tailoring of the dispersion curves. At short wavelengths the modal field remains confined into the silica core region and as the wavelength of light increases, the field penetrates to the air-hole cladding and thus lowers the effective refractive index of the cladding. This unusual interaction of light with air-holes causes unique properties which are not possible to be observed using conventional optical fiber technology.

Recently it was shown by Mangan *et al.* [3], that PCFs can be constructed to behave as an "anti-guide" over certain wavelength range. The refractive index of the core is intentionally decreased by a certain absolute refractive index difference. The lowering mechanism of silica index is achieved through fluorine doping (F-doping). The F-doping lowers the refractive index of core in comparison to the index of undoped-silica region in the cladding and thus the effective cladding index becomes larger than the core index at wavelengths shorter than an "anti-guiding" wavelength λ_a [3]. Therefore, the fiber behaves as an "anti-guide" at all wavelengths shorter than λ_a and can act as a short-wavelength filter. Such a physical property can be employed to improve the coupling characteristics of PCF couplers [4].

On the other hand a fiber coupler is known to be one of the most important components in realizing all-fiber optical communication systems. In this case the light-wave is being transferred sinusoidally between similar cores via a proximity coupling. The coupling characteristics of PCF couplers have been studied extensively in the international literature [5-9]. Polarization-independent PCF wavelength splitters have also been proposed recently [10], based on the inclusion of elliptical air-holes in the cladding of the fiber. However, in all these reports the central problem was the design of dual-core PCF couplers that can operate at one or two distinct wavelengths. Recently, Laesgaard *et al.* [4] have proposed a very interesting design of wavelength-flattened F-doped dual-core PCF coupler, where the two cores were separated by two lattice units. The flattened-coupling length characteristics were obtained for both *x* and *y*-polarizations. Since that time however, no additional efforts have been made to make the device to behave in a polarization-insensitive fashion and moreover the coupling

lengths for x and y-polarizations have not been optimized for achieving reasonable short device length.

Taking all the above circumstances into account, this work adds evidence to the possibility of presenting a systematic design approach for realizing ultra wavelength-flattened dual-core PCF couplers for both x and y-polarizations over a wide bandwidth range. Our proposed strategy for realizing a dual-core F-doped PCF coupler permits us to obtain small coupling lengths for both polarizations. To validate our design, we have adopted an accurate full-vectorial finite element method (V-FEM) modal solver [11], through which we investigate the coupling properties of the newly proposed PCF coupler. Further, an efficient full-vectorial beam propagation method (BPM) [12] is used to justify the polarization-insensitive feature of the device and to verify the results obtained by V-FEM. By an elaborate settlement of the design parameters we have succeeded to optimize the overall physical length of the fiber coupler and also to obtain broader wavelength-flattened characteristics of about 900 nm, in comparison to previously reported dual-core coupler [4].

The present study is organized as follows: In Section 2, we introduce the topology of our proposed PCF structure and we give a priori design guidelines for optimum device performance. Then in Section 3, we introduce the detailed design procedure for obtaining the optimized propagation characteristics of the proposed PCF coupler, based on a trial and error approach and in particular, we propose the elliptically-deformed dual-core shaping as an ingredient for optimum device performance. The impact of the index difference between the fluorine-doping cores and the pure silica is studied in details in Section 4. In Section 5, we present results about the impact of the pitch constant to the overall performance of the proposed device and we estimate its optimized value. Then in Section 6, we estimate the influence of the ellipticity of the air-holes in the cladding of the PCF structure. In Section 7, we study the effect of deforming the shape of the central air-hole which separates the two cores A and B, and we derive its optimum ellipticity. After having derived the optimum structural parameters, in Section 8, we perform BPM simulations for verifying the propagation characteristics previously obtained by the modal analysis and we prove that the coupling characteristics remain very close for both x and y-polarizations, thus we add evidence for the polarization-insensitivity of our design. To address possible limitations regarding the feasibility and the compatibility with standard single mode fibers, in Section 9, we briefly comment on the possibility of realizing our proposed PCF structure and we provide results on splice losses between our proposed PCF coupler and standard optical fibers. Finally in Section 10, we conclude our investigation and we give some possible directions for future work.

2. Architecture of fluorine-doped dual-core PCF coupler with elliptical-deformations

The three-dimensional schematic representation of the PCF structure under consideration, which is composed of elliptical features running along the propagation axis, is shown in Fig. 1. The elliptical air-holes in the cladding of the PCF coupler have major diameters $2r_y$ and minor diameters $2r_x$ and thus the ellipticity is defined as $e = r_y/r_x$, while they are arranged in triangular lattice configuration with lattice constant Λ. The considered PCF has five number of air-hole rings. The fluorine-doped cores A and B represented by red colors, have been perturbed to have elliptical shape with major diameters $2r_{dy}$, and minor diameters $2r_{dx}$, and thus their ellipticity is defined as $e_d = r_{dy}/r_{dx}$. The host material is pure silica with refractive index of 1.45. An efficient V-FEM solver [11] is used to evaluate the effective indices of the super-modes of the dual-core PCF for both x and y-polarizations, assuming no wavelength-dependence of the refractive index of pure silica. The F-doped PCF exhibits a guided mode whose mode field area initially contracts with decreasing wavelength, but at certain threshold begins to expand until antiguiding wavelength is reached [4]. Such unusual variation of mode field area forms the basis of wavelength-flattened broadband directional coupler. The coupling length L_c for a directional coupler at a given wavelength can be derived as

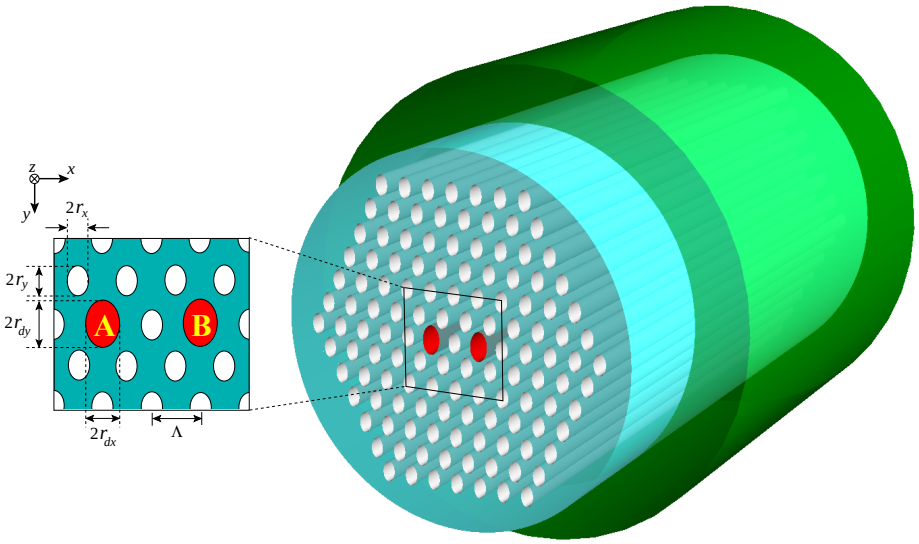

Fig. 1. Schematic representation of the proposed PCF structure. The air-holes in the cladding are arranged in a triangular configuration with lattice constant Λ, major diameters-$2r_y$, and minor diameters-$2r_x$. The dual fluorine-doped cores A and B have been perturbed to have elliptical shape with major diameters-$2r_{dy}$, and minor diameters-$2r_{dx}$, represented by red colors. The host material is pure silica. By a judicious choice of the geometrical parameters, this PCF coupler can exhibit wavelength-flattened coupling characteristics, insensitive to both *x* and *y*-polarizations.

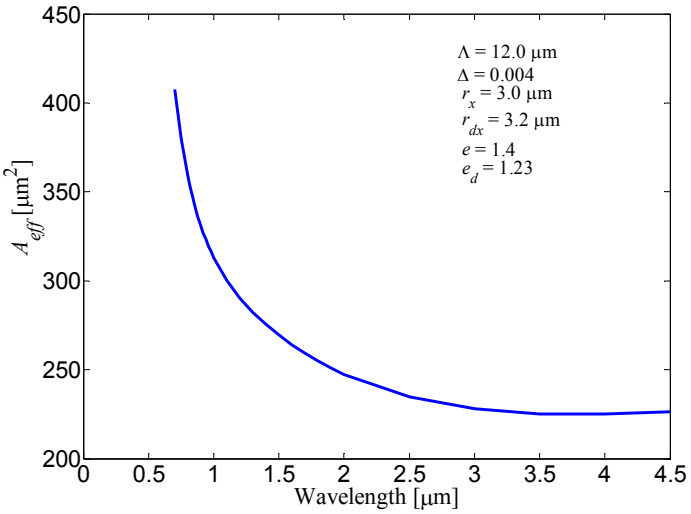

Fig. 2. Variation of the effective mode area of the fundamental guided mode of the F-doped single-core PCF as a function of the wavelength-λ. Contrary to the effective area variation in standard single mode fibers as well as in usual undoped PCFs, we can observe that as the wavelength decreases the effective mode area increases, thus giving rise to the wavelength-flattened coupling characteristics.

$$L_c^{x,y} = \frac{\lambda}{2(n_e^{x,y} - n_o^{x,y})} \tag{1}$$

where $n_e^{x,y}$ and $n_o^{x,y}$ are the effective indexes of *e* (even) and *o* (odd) modes, for *x* and *y*-polarizations respectively, and λ is the operational wavelength. Figure 2 shows the spectral variation of the effective mode area for F-doped single-core PCF with r_y =3.0 μm, e=1.4, r_{dy}=3.2 μm and e_d =1.23, while the pitch constant was chosen initially to be equal with the pitch constant used in [4], that is Λ = 12.0 μm, and the absolute refractive index difference between pure silica and the doped regions was fixed at value of Δ = 0.004. Notice from Fig. 2 that the mode area is initially large at shorter wavelengths and starts to decrease as the wavelength increases and reaches to a certain minimum. The expansion of effective area after reaching to a minimum threshold from longer to shorter wavelengths, for example from 1.7 μm to 0.70 μm, allows the modal fields of both cores to overlap strongly. This enables the reduced and flat coupling characteristics for both *x* and *y*-polarizations.

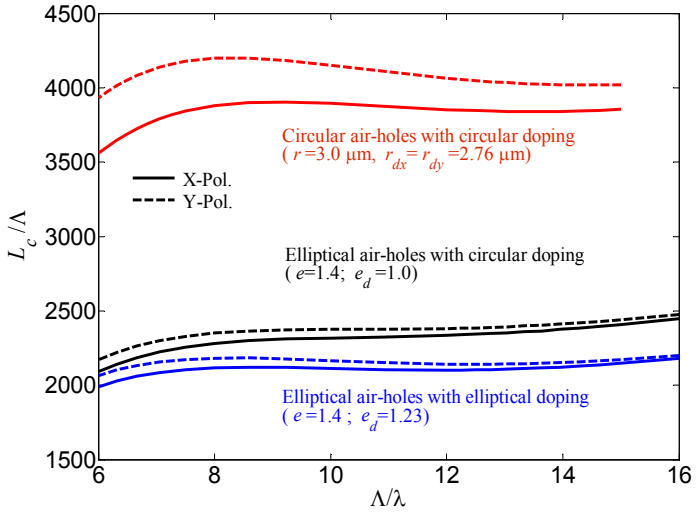

Fig. 3. Normalized coupling length L_c/Λ as a function of the normalized wavelength Λ/λ, for the F-doped dual-core PCF coupler. Solid curves correspond to *x*-polarization while dashed curves correspond to *y*-polarization. Red curves correspond to the results depicted from [4], black curves are associated with elliptically-deformed cladding air-holes having e = 1.4 with circular cores of e_d = 1, while blue curves show the effect of the elliptical-deformation of the doped cores when the ellipticity becomes e_d = 1.23. It is evident from these results that significant reduction of the coupling length can be achieved, by using elliptical features instead of circular.

3. Preliminary design guidelines for optimum device performance

In this section, we present our design approach for achieving optimum characteristics of a wavelength-flattened F-doped, dual-core PCF coupler. Our design approach starts from the design presented in Ref. [4]. The coupling lengths for both polarizations are obtained for a PCF having circular air-holes and circular doped cores as described in Ref. [4], and are plotted in Fig. 3 (red curves). The solid and dashed curves in Fig. 3, represent the variation of the normalized coupling length L_c/Λ for *x* and *y*-polarizations respectively, as a function of the normalized wavelength Λ/λ. It can be clearly seen from Fig. 3, that the normalized coupling lengths as well as the difference between the coupling lengths for both *x* and *y*-polarizations

for the initial design reported in Ref. [4], is quite large, which is due to the fact that the resulting core configuration is directed across the *x*-axis [7]. In order to reduce the level of the coupling lengths and also the difference between the two polarized partial coupling lengths, we consider the case of incorporating elliptical air-holes in the cladding, with an ellipticity of e=1.4 (r_y=3.0 μm) and circular doping regions as in the former case [4]. The results obtained in this case are shown in Fig. 3 with black curves. From these results it becomes clear that the magnitude of the coupling length for the same pitch and the same circular doping region is reduced to almost half of their initial values. This is due to a stronger overlap of the modal fields between the two cores, which is realized by elongating the air-holes across the *y*-direction by shortening them across the *x*-direction.

Then we proceed by varying the shape of the doping region uniformly from circular to elliptical. For a fixed doped ellipticity (e_d = 1.23, r_{dy} = 3.2 μm), we found that the coupling lengths can be reduced further as well as the difference between the partial coupling lengths for both *x* and *y*-polarizations (shown by blue colored curves in Fig. 3). While on the other hand the bandwidth of the flat coupling lengths can be broadened by a factor of about 150 nm in comparison to the resulted bandwidth of 750 nm reported in [4], thus giving a total of 900 nm flat bandwidth. The difference between the partial coupling lengths corresponding to *x* and *y*-polarizations, is reduced due to the high birefringence offered by the presence of elliptical air-holes in the cladding of the PCF structure as proposed in [13, 14].

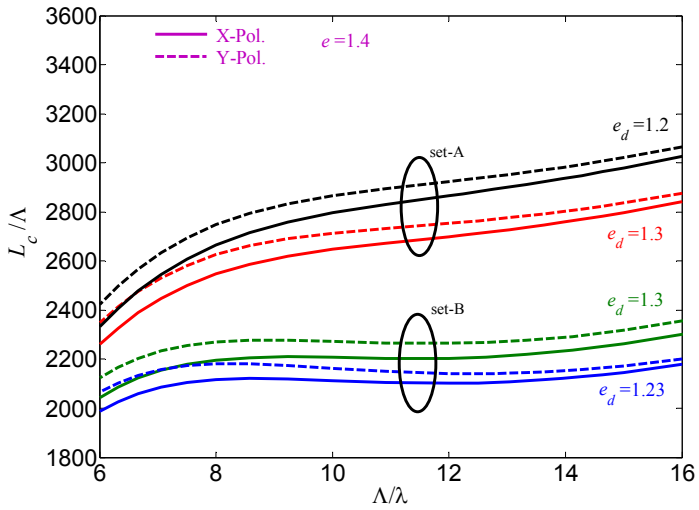

Fig. 4. Normalized coupling length L_c/Λ as a function of the normalized wavelength Λ/λ, for the F-doped dual core PCF coupler, and for two different sets of doping ellipticities that is: Set A (black and red curves), and Set B (blue and green curves). Solid curves correspond to *x*-polarization while dashed curves correspond to *y*-polarization. From these results becomes evident that by controlling the ellipticity of the doped regions we can succeed having optimum ultra-flat coupling characteristics (corresponding to blue curves) and additionally the total bandwidth was enlarged by a factor of 150 nm in comparison to the results in [4].

As a next step, we confirm that the selection of the previous mentioned doped cores ellipticity of e_d = 1.23 is the optimum one. To do this, we consider two different cases (sets of design parameters), while we keep the following parameters fixed: Δ = 0.004, e =1.4 (r_y= 3.0 μm) and Λ = 12.0 μm: Set-A: (i) r_{dx} = 2.3 μm, r_{dy} = 2.76 μm, e_d = 1.2 (black curves), and (ii) r_{dx} = 2.123 μm, r_{dy} = 2.76 μm, e_d = 1.3(red curves). Set-B: (i) r_{dx}=2.6 μm, r_{dy}=3.2 μm, e_d = 1.23 (blue curves), and (ii) r_{dx} = 2.461 μm, r_{dy} = 3.2 μm, e_d = 1.3, (green curves). It should be noticed that in the Set-A, the dimensions of the elliptically-deformed doped core regions are

different than those in Set-B, even though the ellipticity remains same. The variation of the normalized coupling lengths for both polarizations is plotted in Fig. 4 as a function of the normalized wavelength. It can be concluded from the results in Fig. 4 that for the design parameters in Set-A, the coupling length is not anymore flat. If we alter the length of major and minor axis of the doped regions as in Set-B (i) and (ii), we can clearly see that at first the normalized coupling lengths for both polarizations decrease further and if we decrease the ellipticity of the doped region (Set-B (ii) shown by blue curves), we can succeed in obtaining more flattened coupling lengths with improved bandwidth broadness. Therefore, from the above analysis it can be concluded that by a precise control of the doped region's ellipticity, broadband flat coupling lengths can be realized.

4. Influence of the index difference between the fluorine doped region and pure silica

In this section, we study the impact of the doping refractive index on the coupling length characteristics of the proposed PCF device. The absolute refractive index difference Δ is varied from 0.001 to 0.006 with a step of 0.001, for fixed doping region ellipticity as confirmed previously (Set-B(ii)), cladding air-hole ellipticities e =1.4 with r_y=3.0 μm, and pitch constant Λ=12 μm. The variation of the normalized coupling length as a function of the normalized wavelength for different Δ is shown in Fig. 5. For the lowest doping index difference, that is $\Delta = 0.001$, the coupling lengths for both x and y-polarizations are not flat (solid and dashed cyan colored curves). As the doping index difference increases, the coupling lengths continuously decrease, and additionally we observe a remarkable flatness. There is a certain value of the index difference-Δ after which, although we observe further decrement of the coupling length, the flatness however is destroyed. This value was derived to be $\Delta = 0.004$. As a conclusion we can say that for a fixed doping difference of $\Delta = 0.004$, the flatness as well as the small coupling lengths and small coupling length difference corresponding to polarization-insensitive feature can be achieved (shown in Fig. 5 by the blue curves).

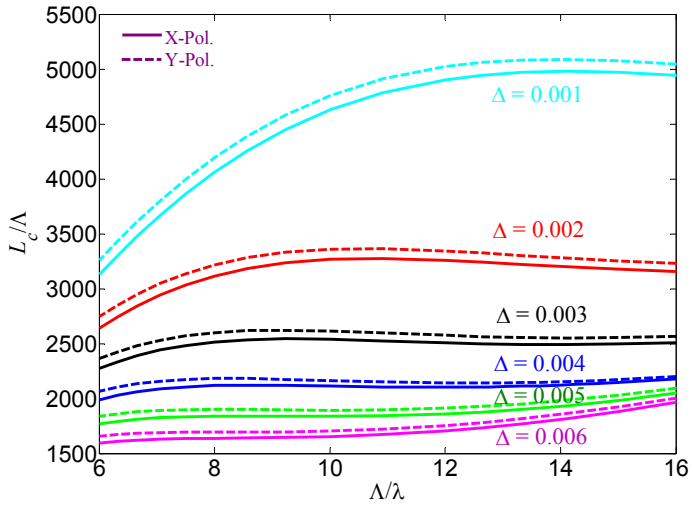

Fig. 5. Normalized coupling length L_c/Λ as a function of the normalized wavelength Λ/λ, for the F-doped dual-core PCF coupler, for different incremental index differences between the doped-cores and the host material (pure silica). It is clear that by increasing the index difference the coupling length decreases while at the same time the flatness improves drastically. There is a value of the index difference where the optimum flatness occurs. This optimum value has been estimated to be $\Delta = 0.004$ (blue curves).

5. The effect of the pitch constant variation on the overall PCF performance

From the point of view of the fabrication feasibility of the designed PCF coupler, pitch constant may vary within ±2 % around its nominal value as was recently demonstrated experimentally in Ref. [15]. Therefore, at this stage we numerically evaluate the effect of the pitch constant variation, on the coupling lengths of the proposed PCF coupler. We set the fiber's parameters as stated by set-B (ii) (i.e. e_d=1.23 and r_{dy}=3.2 μm), cladding air-hole ellipticities e =1.4 (r_y=3.0 μm), and Δ = 0.004. The pitch constant is assumed to vary within ±2 % in the vicinity of Λ = 12.0 μm. The normalized coupling lengths for both polarizations are displayed in Fig. 6 as a function of the normalized wavelength. The red curves correspond to −2 % from its nominal, showing that by decreasing the pitch constant, the partial coupling lengths increase, while at the same time the flatness is getting worst. In contrary, when the pitch constant increases, the coupling lengths decrease with additional reduction of their flat bandwidth. As a conclusion we can say that the selection of the initial pitch constant of Λ = 12.0 μm generates the best coupling length characteristics. On the other hand we should notice that a possible tolerance of this parameter may drastically affect the flat behavior of the coupling characteristics. As a general rule the fabrication tolerances should be kept below ±1 % in order to ensure the smooth feasibility of the proposed PCF coupler in large quantities.

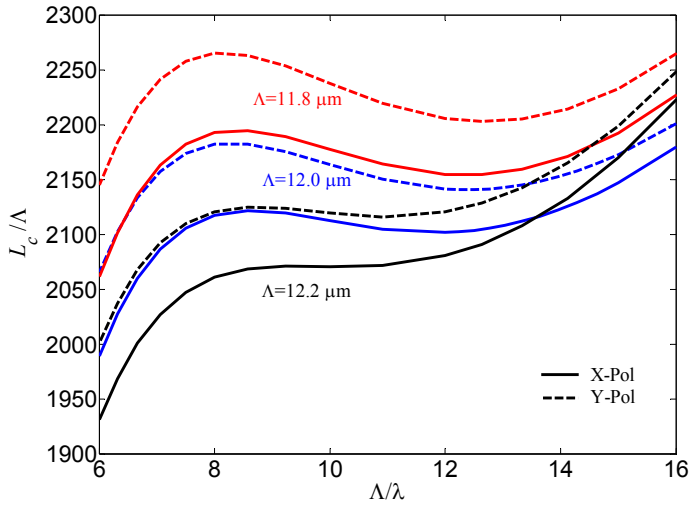

Fig. 6. Normalized coupling length L_c/Λ as a function of the normalized wavelength Λ/λ, for the F-doped dual-core PCF coupler, for a ±2 % tolerance of the pitch constant. From these results we can see that indeed the variation of the coupling length seems sensitive to possible variations of the pitch constant. Additionally we confirm that the optimum value of the pitch constant for achieving the best flatness is Λ = 12 μm.

6. The impact of the elliptically-deformed cladding air-holes

During the fabrication process, we may also expect the statistical deformation of the air-holes in the cladding in the same manner as with the pitch constant. So this section is devoted to study in a more detailed way the possible impact of the variable ellipticity of the air-holes in the cladding of the proposed PCF coupler. Again we assume that the initial optimized selection of the ellipticity of the air-holes in the cladding varies by a tolerance of ±2 % from its nominal value, that is e =1.4. The effect of the fluctuation in the cladding air-holes ellipticity on the partial coupling lengths for both polarizations is shown in Fig. 7, where

results showing by red curves correspond to decreased ellipticity of e =1.38 keeping the value of r_y=3.0 μm and varying the r_x, while black curves correspond to increased ellipticity of e =1.42. The initial optimized coupling characteristics are shown by the blue curves, for x-polarization (solid curve), and y-polarization (dashed curve). It can be revealed from Fig. 7 that the coupling lengths become larger for smaller ellipticities of the air-holes in the cladding, while when the ellipticity increases the coupling lengths for both polarizations decrease. The physical explanation of these results is that by decreasing the ellipticity of the air-holes in the cladding, the interaction of modal fields between the two cores A and B becomes weaker compared with an increased ellipticity. In addition we can clearly observe that the flatness is reduced but by a smaller factor in comparison to the impact of the pitch constant. As a general conclusion we can fairly say that the ellipticity variation of the air-holes in the cladding of the proposed PCF coupler is not a dominant factor for drastical changes in the coupling characteristics.

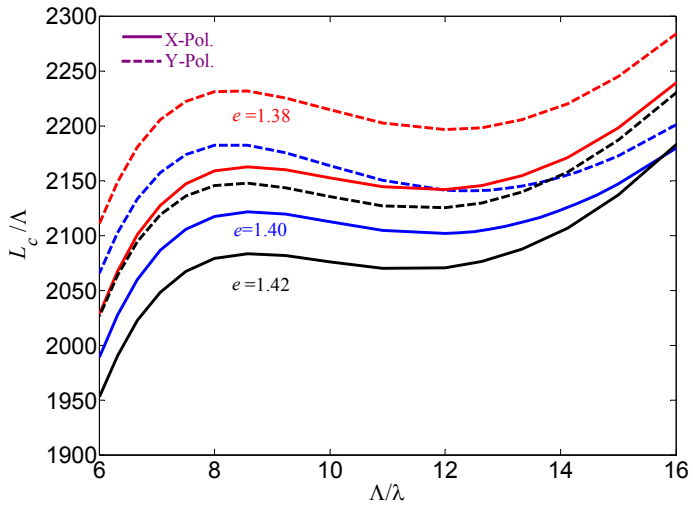

Fig. 7. Impact of the variation of the cladding's air-holes ellipticity-e to the normalized coupling length L_c/Λ, as a function of the normalized wavelength Λ/λ for the F-doped dual-core PCF coupler. Solid curves correspond to x-polarization while dashed curves to y-polarization. The tolerance was chosen as ±2 % around its nominal value of e = 1.4.

7. The impact of the elliptically-deformed central air-hole separating the two cores

In the previous discussion it became evident that the key factor for reducing the coupling lengths for this type of PCF coupler, while at the same time we keep the ultra-flat propagation characteristics over a wide wavelength range, is the dynamic controllability of the modal field interaction between the two cores. A parameter which can further strengthen or weaken this interaction is the ellipticity of the central air-hole, which separates the two cores A and B. So in this section we study in details the possible influence of the central air-hole ellipticity variation on the derived optimum coupling lengths for both polarizations. The central air-hole ellipticity is assumed to change within a range of ±1 % and ±2 % from its initial derived value by varying r_y and keeping r_x constant. All the other design parameters were fixed in their optimum value. The results from this variation are shown in Fig. 8, where in particular the results presented with blue curves correspond to the optimum characteristics, green curves correspond to an increased ellipticity by a factor of +2 %, red curves correspond to an increased ellipticity by a factor of +1 %, purple curves correspond to a decreased ellipticity by

a factor of –1 %, and finally black curves correspond to a decreased ellipticity by a factor of –2 %. From the results presented in Fig. 8 we can conclude that by decreasing or increasing the ellipticity of the central air-hole which separates the two cores A and B, the difference between the partial coupling lengths for *x* and *y*-polarizations increases, thus the polarization-insensitive coupling becomes poor. Additionally the continuous decrement of the ellipticity of the central air-hole can reduce further the values of the normalized coupling lengths because the interaction between the two cores becomes stronger. Therefore as a conclusion we can say that for keeping the insensitiveness of the polarization the central air-hole should be kept by all means same as the air-holes in the cladding. The same tendency of the coupling curves was confirmed also for the opposite scenario where we keep r_y constant and vary r_x.

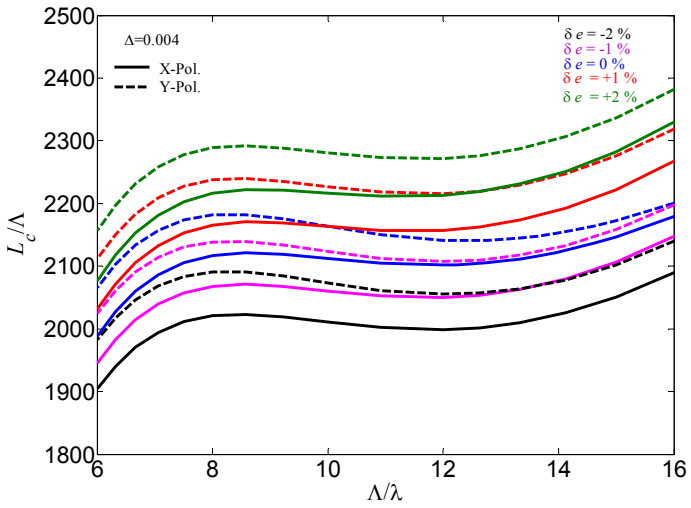

Fig. 8. Influence of the ellipticity tolerance of ±1 % and ±2 % around its nominal value of e = 1.4 of the central air-hole (i.e. the air-hole which separates the two cores), for *x*-polarization (solid curves), and *y*-polarization (dashed curves). It is evident that when the ellipticity increases the coupling length increases while the flatness becomes poor. As a conclusion the central air-hole ellipticity should be the same with the ellipticity of the air-holes in the cladding.

8. BPM simulation results and coupling length verification

After having derived the optimized PCF structural parameters through the design approach presented in Sections 2 to 7, we perform BPM simulations [12] for confirming the exact values of the partial coupling lengths as well as to justify the bandwidth over which polarization-insensitive characteristics are obtained. We have particularly chosen to use an accurate BPM simulator for independently confirm the obtained results, which could have been derived by the modal analysis using an accurate V-FEM solver presented in previous sections. The normalized power characteristics at wavelength of 1.55 μm are obtained as a function of the propagation distance for both *x* and *y*-polarizations in Figs. 9(a) and (b) respectively, where blue curves represent the coupling characteristics of core-A which is considered to be the input core and red curves represent the coupling characteristics of core-B, which is considered to be one of the output core. It can be clearly seen from Fig. 9(a) that the power splits into half after traveling a distance equal to a coupling length of L_c =12.68 mm, for *x*-polarized mode. For *y*-polarized mode the coupling length was obtained to be L_c = 13.07 mm, as shown in Fig. 9(b). The slightly difference between the two partial coupling lengths is due to the fact that the formation of the two adjacent cores was done by eliminating air-holes

in an array across the x-axis. In Fig. 10 we plot the normalized power variation for (a) x-polarization and (b) y-polarization as a function of the operating wavelength and for fixed coupling length of L_c = 13 mm. From these results we can conclude that by choosing the overall coupling length to be L_c = 13 mm, we can obtain a 50 % power splitting between the two cores within a fluctuation of ±1 %. This means that our proposed PCF coupler will operate as an effectively 3-dB coupler with an uncertainty in the power level of ±1 % between the two cores, a level which can be considered acceptable for most practical applications.

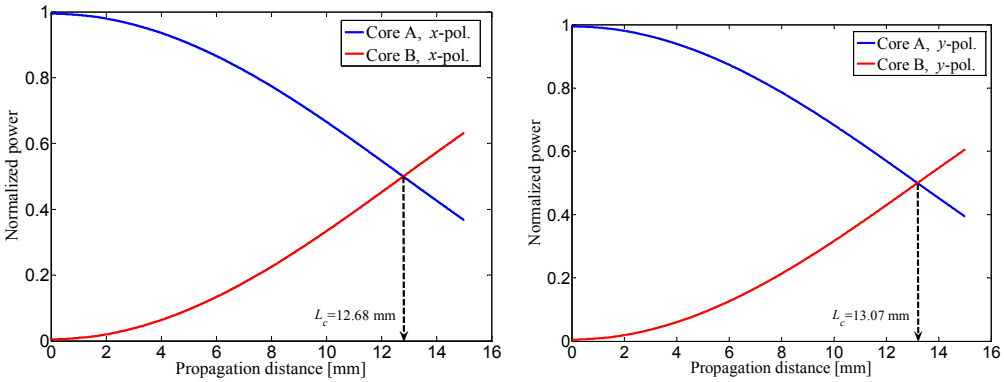

(a) (b)

Fig. 9. Normalized power variation inside the dual-core PCF coupler as a function of the propagation distance at wavelength of 1.55 μm, for (a) x-polarization, (b) y-polarization and for core-A (blue curve), core-B (red curve). The coupling lengths have been confirmed by the BPM analysis to be L_c = 12.68 mm for the x-polarized mode and L_c = 13.07 mm for the y-polarized mode. The slightly difference between the two partial coupling lengths comes from the orientation of the two cores across the x-axis.

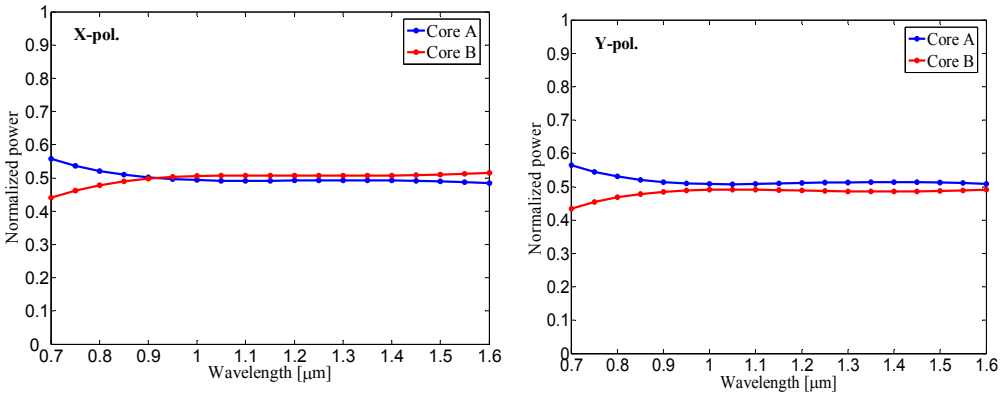

(a) (b)

Fig. 10. Normalized power variation inside the dual-core PCF coupler as a function of the operating wavelength in the dual-core PCF coupler calculated at fixed coupling length of L_c = 13 mm, for (a) x-polarization and (b) y-polarization. The blue curve corresponds to the output power in core-A, while the red curve corresponds to core-B. The main conclusion from these results is that the coupling efficiency varies by a fraction of ± 1 % in the wavelength range from 0.9 μm up to 1.6 μm, around the expected value of 0.5 corresponding to the operation of a 3-dB coupler.

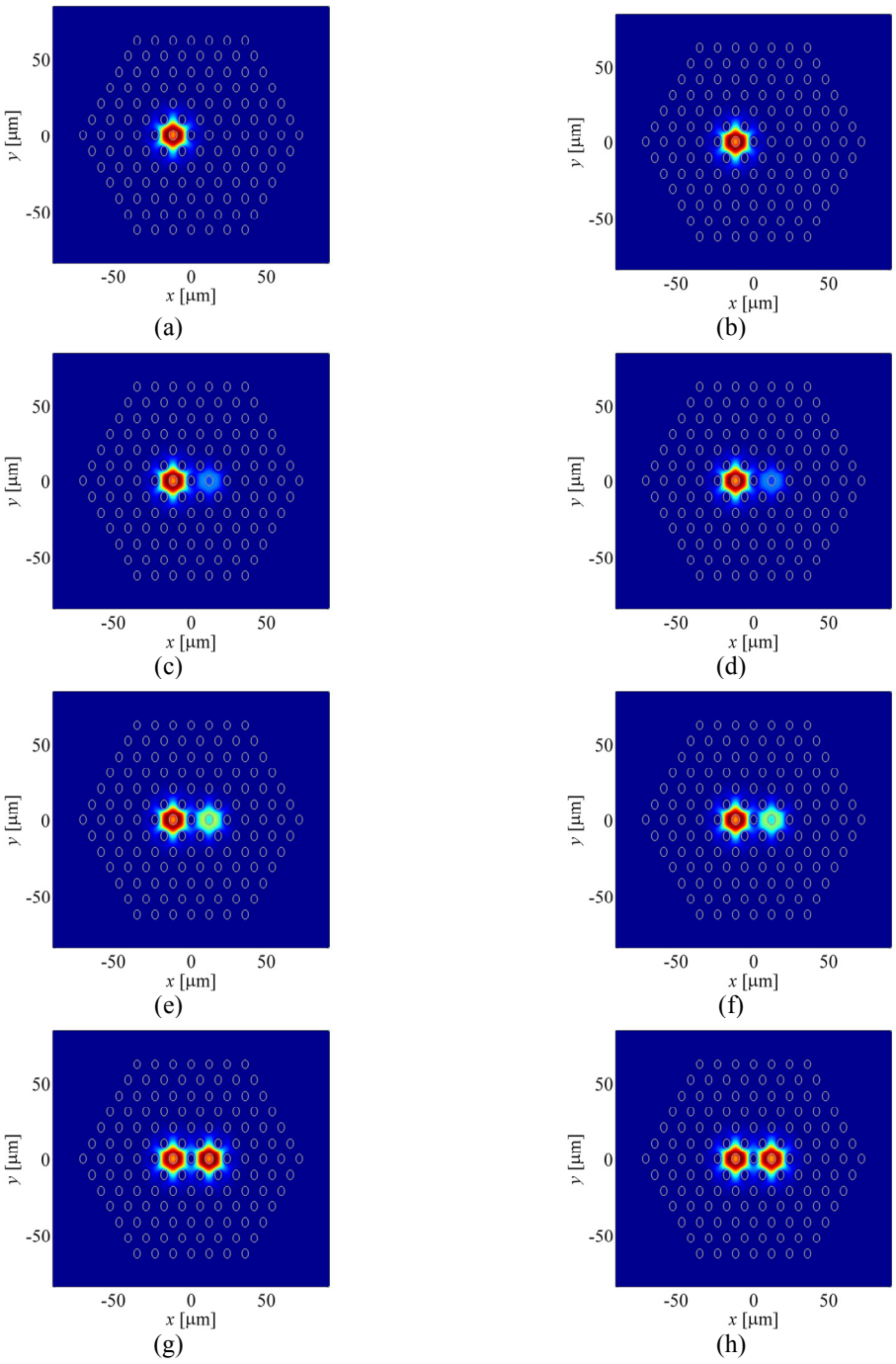

Fig. 11. Snapshots of the electric field distribution, at a fixed wavelength of λ = 1.55 μm in the proposed polarization-insensitive dual-core F-doped PCF coupler calculated by the BPM analysis, for (a) *x*-polarized mode (E_x) and (b) *y*-polarized mode (E_y) at distance of z = 0 mm, (c) *x*-polarized mode (E_x) and (d) *y*-polarized mode (E_y) at a distance of 4 mm, (e) *x*-polarized mode (E_x), and (f) *y*-polarized mode (E_y) at a distance of 8 mm, and (g) *x*-polarized mode (E_x), and (h) *y*-polarized mode (E_y) at a distance of 13 mm. At the coupling length of L_c = 13 mm the power was splitted in the two cores within a difference of ± 1 %. Thus the device effectively acts as a polarization-insensitive 3-dB coupler.

In addition we can justify the wavelength range over which polarization-insensitiveness can be obtained. From Figs. 10(a) and (b) we can see that between 0.9 μm and 1.6 μm wavelength range the splitting power remains within ±1 % from the targeted value of 50 %. This 700 nm wavelength range for the polarization-insensitive 3-dB PCF coupler is reported for the first time.

To visualize the power splitting mechanism in our proposed PCF coupler, in Fig. 11 we show the propagation characteristics obtained by an accurate BPM analysis [12]. Specifically Fig. 11 shows the snapshots of the electric field distribution, at a fixed wavelength of $\lambda = 1.55$ μm, for (a) *x*-polarized mode (E_x) and (b) *y*-polarized mode (E_y) at a distance of $z = 0$ mm, (c) *x*-polarized mode (E_x) and (d) *y*-polarized mode (E_y) at a distance of 4 mm, (e) *x*-polarized mode (E_x), and (f) *y*-polarized mode (E_y) at a distance of 8 mm, and (g) *x*-polarized mode (E_x), and (h) *y*-polarized mode (E_y) at a distance of 13 mm. We can clearly observe that at the coupling length of $L_c = 13$ mm the power was splitted in the two cores A and B within a power fluctuation of ± 1 % from the targeted level of 50 %. Thus our proposed PCF device effectively behaves as a polarization-insensitive 3-dB coupler over a wide wavelength range, specifically from 900 nm to 1600 nm. The reduced coupling length of $L_c = 13$ mm is the main advantage of the proposed optimized design in comparison to the previously reported coupler [4], where the overall coupling length was derived to be $L_c = 27$ mm. Additionally our device was designed to exhibit polarization-insensitive propagation characteristics, thus it can be used for both *x* and *y*-polarized signals.

9. Feasibility and compatibility of the proposed PCF coupler

Although the objective of this paper was the theoretical design of this polarization-insensitive dual-core PCF coupler, at this point we wish to address some issues regarding the technological feasibility and the compatibility with standard single mode fibers (SMF) of our proposed PCF coupler. Very recently, it came to our attention that elliptical air-hole PCFs with high birefrigent properties have been successfully fabricated and measured in Ref. [16]. Elliptically-shaped Ge-doped core polarization-maintaining PCFs, exhibiting dispersion-flattened characteristics have been successfully fabricated and measured in Ref. [17]. Regarding possible bending losses, the compact size of our PCF device prohibits the bending operation and therefore bending losses are not an issue in this PCF coupler. The next task is to consider how efficiently we can couple light in this new type of wavelength-flattened PCF coupler. According to our investigations, perhaps the best way to couple light in this PCF device is by splicing to a standard SMF and then launching the light from a laser source direct to SMF. This approach is very effective for making low-loss interface between an SMF and a PCF as was recently pointed out experimentally [18]. In such case however the fields between the elliptically-shaped cores and the circular-shaped SMFs are to a certain extent mismatched and therefore unavoidable splice losses may arise. A possible solution to this problem would be the use of elliptically-shaped SMFs to match exactly the modal fields of the elliptically-deformed dual cores. In order to justify the compatibility with standard optical fibers we have performed splice loss calculations between our proposed PCF coupler and a standard SMF with core diameter 10 μm and relative index difference Δ=0.3%. From the results in Fig. 12, we may conclude that the splice loss is large for short wavelengths while it decreases as the wavelength increases. This is due to the fact that the effective mode area decreases as the wavelength increases because the light is more confined into the fluorine doped region. Notice that the splice loss is almost identical for both *x* and *y*-polarizations, which indicates the polarization insensitive behavior of our proposed design. Although the splice loss is found to be high at shorter wavelengths, one way to reduce further the splice loss is by using an intermediate buffer SMF [19] with mode field diameter between the fluorine-doped single core PCF and the standard SMF. As a conclusion of this section we can fairly say that our proposed PCF coupler has no serious integration issues with other optical fiber devices. As for the realization of the proposed PCF device at the present state may be a bit tedious, however it

is certainly a technological challenge for the experimentalists, and we hope that in the near future our device can be fabricated and its true performance can be verified experimentally.

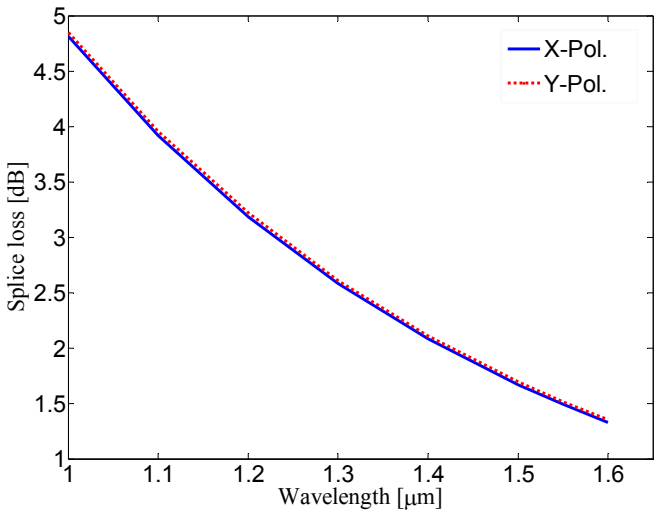

Fig. 12. Variation of splice loss as a function of the wavelength for *x*-polarization (blue solid curve) and *y*-polarization (red dotted curve). It can be clearly seen that the splice loss decreases as wavelength increases. Note that the splice loss is almost identical for both *x* and *y*-polarizations a fact that indicate the polarization insensitivity of the proposed design.

10. Summary

To conclude our investigation, we have presented a thorough design approach for optimizing the propagation characteristics of dual-core F-doped PCF couplers with elliptically-deformed features, such as elliptical cladding air-holes and elliptically-deformed doped-cores. Our results have confirmed the optimized properties of the proposed structure, in comparison to previous works [4]. Specifically we have succeeded in the following device performance: wavelength-flattened coupling characteristics with an enlarged bandwidth of 150 nm, polarization-insensitive characteristics for both *x* and *y*-polarizations as well as power coupling ratio of 50±1 % in the wavelength range: 0.9 μm to 1.6 μm. Additionally the overall coupling length was reduced to half of its initial obtained value in Ref. [4]. Extensive numerical results regarding the impact of all possible design parameters have been shown and the device performance was also verified by an accurate BPM analysis. We believe that the inclusion of elliptically-deformed features in different PCF structures can generate certain intriguing propagation characteristics; therefore the inclusion of elliptical features for realizing various PCF devices is an active research topic in our group.

Acknowledgements

The authors would like to acknowledge to 21st Century COE (Center of Excellence) program: Meme-Media Technology Approach to the R&D of the Next Generation Information Technologies. We also would like to sincerely thank Jesper Laegsggard from the Technical University of Denmark for providing us useful technical information regarding PCF couplers.